



ISSN: 2617-6548

URL: [www.ijirss.com](http://www.ijirss.com)

## A study on a hydrogen injection control method for fuel cell engines based on proportional valve polling

Ge Lixia<sup>1\*</sup>, Mohammad Nizamuddin Inamdar<sup>2</sup>, Aiman Alodainia<sup>3</sup>

<sup>1,2,3</sup>Lincoln University College, Petaling Jaya 47301, Malaysia.

Corresponding author: Ge Lixia (Email: [lixia.phdscholar@lincoln.edu.my](mailto:lixia.phdscholar@lincoln.edu.my))

### Abstract

As the core component of fuel cell engine hydrogen supply systems, hydrogen injection solenoid valves suffer from high switching frequency, excessive power consumption and shortened service life under traditional equal-distribution control, which raises system failure risks and maintenance costs. To solve these problems, this paper puts forward a polling control strategy based on PI closed-loop pressure regulation. The stack inlet hydrogen pressure is sampled in real time to calculate the overall hydrogen injection duty cycle, which is evenly assigned to six solenoid valves via sequential allocation and cyclic rotation to balance valve workload and cut single-valve actuation frequency and heat loss. Co-simulation of Simulink and AMESim is conducted to compare three control modes, and a durability test bench is built for experimental validation. The Parker model is adopted to evaluate valve life attenuation. Simulation and test results reveal that the proposed polling method effectively suppresses hydrogen pressure fluctuation under low-flow conditions and improves control accuracy. It reduces valve switching times, power consumption and operating temperature, slowing insulation and seal aging. Durability tests show its first-failure time and total service life exceed the equal-distribution mode by over 2.5 times with fewer faulty valves. This strategy optimizes pressure control and component durability, offering great engineering application value for long-life commercial fuel cell vehicles.

**Keywords:** Hydrogen supply system, Hydrogen injection valve, Polling control, Co-simulation, Durability life.

**DOI:** 10.53894/ijirss.v9i7.11789

**Funding:** This study received no specific financial support.

**History: Received:** 24 March 2026 / **Revised:** 5 June 2026 / **Accepted:** 9 June 2026 / **Published:** 6 July 2026

**Copyright:** © 2026 by the authors. This article is an open access article distributed under the terms and conditions of the Creative Commons Attribution (CC BY) license (<https://creativecommons.org/licenses/by/4.0/>).

**Competing Interests:** The authors declare that they have no competing interests.

**Authors' Contributions:** All authors contributed equally to the conception and design of the study. All authors have read and agreed to the published version of the manuscript.

**Transparency:** The authors confirm that the manuscript is an honest, accurate, and transparent account of the study; that no vital features of the study have been omitted; and that any discrepancies from the study as planned have been explained. This study followed all ethical practices during writing.

**Publisher:** Innovative Research Publishing

### 1. Introduction

With the advancement of hydrogen energy technology, fuel cell engines are increasingly applied in transportation and energy sectors [1]. Current fuel cell engine lifespan requirements range from 25,000 to 30,000 hours, while the "Energy-

saving and New Energy Vehicle Technology Roadmap 2.0" explicitly sets a commercial vehicle lifespan target of 30,000 hours by 2035 [2]. As a critical component of hydrogen fuel engine supply systems, the reliability of hydrogen injection solenoid valves directly impacts engine durability and subsequent maintenance costs. Operational data indicates that primary failure modes include leakage, failure to operate, and sticking, with seal failure being particularly prominent. This primarily stems from the aging of rubber materials like O-rings under high-temperature and high-frequency conditions, where temperature serves as a key accelerating factor Guo, et al. [3] and Liu and Zhou [4]. Angadi, et al. [5] summarized research progress on critical operational characteristics of solenoid valves, including reliability, performance, and remaining life, with particular emphasis on the impact of coil insulation Angadi and Jackson [6]. Hou, et al. [7] developed an effective fatigue life assessment method for solenoid valves under different module operating conditions based on statistical results and experimental testing of valve actuation cycles Hou, et al. [7]. Li, et al. [8] utilized Ansys finite element software to establish an electromagnetic valve model, incorporating temperature loads into the mechanical stress field solution. This yielded a stress field under coupled mechanical and thermal stresses, revealing a gradual coil failure mechanism Li, et al. [8]. Tao and Ma [9] employed finite element technology to simulate fatigue life calculations for spring components in high-speed response electromagnetic valves Tao and Ma [9]. Mazaev, et al. [10] employed a Bayesian convolutional neural network to predict the remaining service life of solenoid valves by training on their current characteristic curves [10].

Current research primarily focuses on individual solenoid valve failure mode studies and life assessment calculations. This paper proposes a collaborative control method for solenoid valve groups from a control perspective, tailored for hydrogen fuel engine applications. This approach aims to reduce switching frequency, on-time duration, and power consumption, thereby extending solenoid valve lifespan and improving hydrogen pressure control performance. It provides a technical pathway for high-reliability hydrogen supply systems.

## 2. Principle of the Injection Hydrogen Supply System

As shown in Figure 1, the hydrogen supply system for a hydrogen fuel cell engine comprises a high-pressure hydrogen storage tank, a pressure-reducing valve, a hydrogen injection solenoid valve assembly, a drain valve, and associated piping. Hydrogen is pressurized and stored in the high-pressure tank. During engine operation, hydrogen from the tank is reduced to the target pressure via the pressure reducer valve, then undergoes precise flow regulation through the hydrogen injection solenoid valve assembly to meet the fuel cell stack's hydrogen demand under varying operating conditions. Throughout this process, the drain valve effectively expels accumulated condensate and exhaust gases from the system, ensuring stable operation and high efficiency. However, this may cause fluctuations in hydrogen flow and pressure, necessitating regulation by the hydrogen injection solenoid valve assembly to suppress such variations.

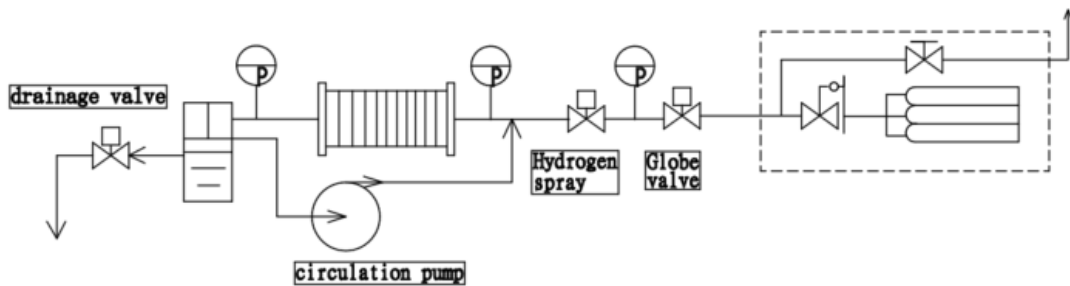


Figure 1. Hydrogen Supply System for Hydrogen Fuel Cell Engine.

### 2.1. Operating Principle of the Hydrogen Supply Assembly

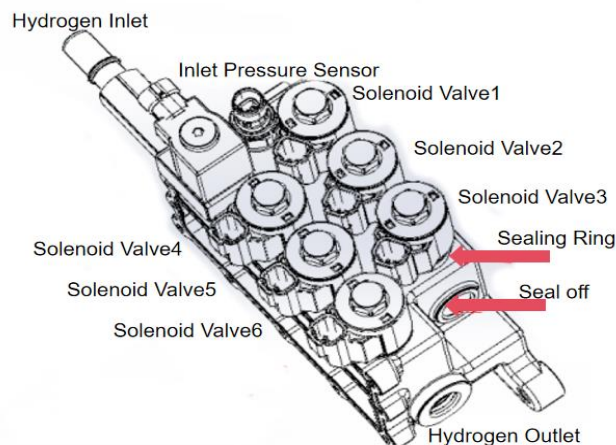
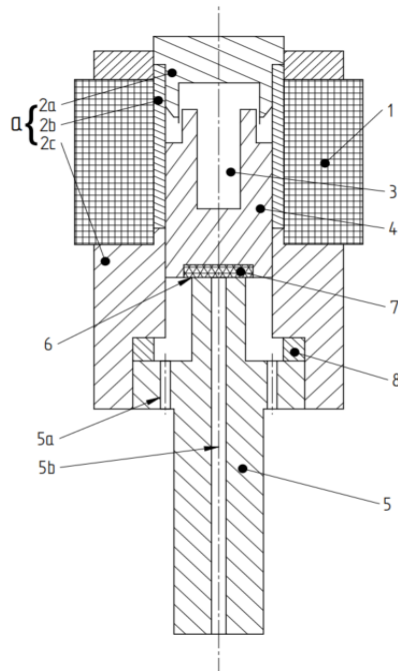


Figure 2. Hydrogen Supply Assembly.

This study examines the hydrogen supply assembly of a 120kW hydrogen fuel cell system, as shown in Figure 2. This assembly integrates a shut-off valve, inlet pressure sensor, and six solenoid valves. During operation, the shut-off valve remains open, with the six solenoid valves collectively regulating hydrogen flow rate and the assembly's outlet pressure (stack inlet pressure). The solenoid valves employ a common rail design, ensuring equivalent regulation effectiveness across all six valves within the assembly.



**Figure 3.**  
Solenoid Valve.

As shown in Figure 3, the hydrogen injection solenoid valve consists of a coil 1 , lock nut 2a , magnetic shield sleeve 2b , base 2c , armature spring 3 , armature 4 , valve body 5 , and sealing gasket 8 .Hydrogen enters through inlet 5a. When coil 1 energizes, armature 4 moves upward under electromagnetic force, overcoming the spring force of armature spring 3. This opens sealing surfaces 6 and 6 between the lower face of armature 4 and the top of valve body 5, allowing gas to flow out through outlet 5b to the fuel cell inlet.

Solenoid valve parameters are as follows:

**Table 1.**  
Solenoid Valve Parameters.

Item	Parameter	Item	Parameter
Drive Voltage	DC24V	Coil Resistance	$6 \pm 5\% \Omega$
Drive Method	PWM (Peak-Hold)	CV Value	0.07
Drive Frequency	10-50Hz	Drive Current	Peak: 3.5A; Hold: 1.5A–1.8A

### 3. Control Scheme Design

To achieve superior hydrogen pressure control performance and extend the assembly's service life, the control scheme design is illustrated in Figure 4. This scheme comprises three components: PI control, target duty cycle allocation, and command polling.

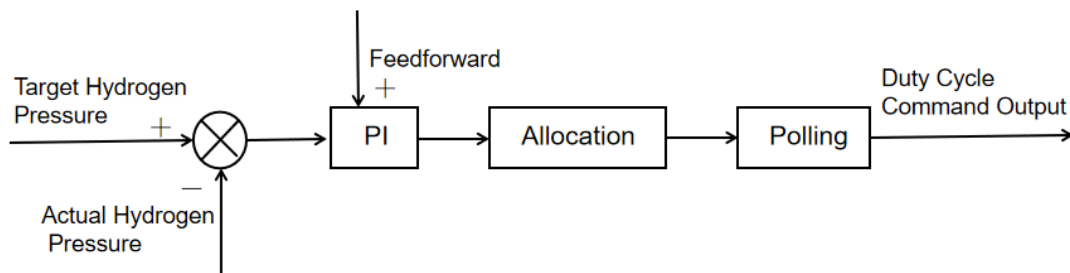


**Figure 4.**  
Control Strategy Diagram.

### 3.1. Hydrogen Pressure PI Feedforward Control

Real-time monitoring of actual hydrogen inlet pressure via pressure sensors calculates the difference between target pressure ( $P_{set}$ ) and actual pressure ( $P_{actual}$ ) as input to the PI controller, enabling feedforward compensation for disturbances under varying operating conditions. The PI algorithm then calculates the total target duty cycle. This calculated duty cycle is distributed among the individual hydrogen injector solenoid valves to regulate the hydrogen flow through each valve, achieving closed-loop control of the assembly outlet pressure (hydrogen inlet pressure).

Reactor-entry hydrogen pressure error signal  $e(t)$ :

$$e(t) = P_{set} - P_{actual} \quad (1)$$

PI output:

$$u(t) = K_p e(t) + K_i \int_0^t e(t) dt + \delta(t) \quad (2)$$

Where:  $u$  -- Total duty cycle output,  $K_p$  -- Proportional coefficient,  $K_i$  -- Integral coefficient,  $\delta$  -- Feedforward compensation.

This controller primarily compensates for pressure fluctuations caused by the operation of the hydrogen line venting/drain valve. According to the relevant drain valve specification sheet, the flow rate is 70 SLPM when the inlet air pressure is 1 bar and the outlet pressure is 0 bar. Assuming the temperature at the tail vent is the same as at the inlet of the hydrogen spray solenoid valve, the compensation during drain valve operation is:

$$\delta(t) = 0.118 * P1/P2 * \sqrt{273 * G2/G1} \quad (3)$$

Where:  $P1$  -- kPa.A: Tailpipe valve inlet pressure,  $P2$  -- kPa.A: Hydrogen spray solenoid valve inlet pressure,  $G1$  -- Specific gravity of tailpipe exhaust gas,  $G2$  -- Specific gravity of hydrogen gas.

### 3.2. Target Duty Cycle Allocation

The total solenoid valve duty cycle obtained in Section 3.1 must be allocated among individual valves. An equal distribution would cause all valves to operate synchronously throughout the system cycle, remaining active at all times. Frequent switching accelerates reaching the valve's switching endurance limit, reducing its service life. Additionally, the solenoid valves employ a Peak-Hold drive mode, requiring each valve to maintain a minimum duty cycle to prevent activation failure. Therefore, equal distribution during low-flow demand can cause flow fluctuations, increasing control complexity and system risk.

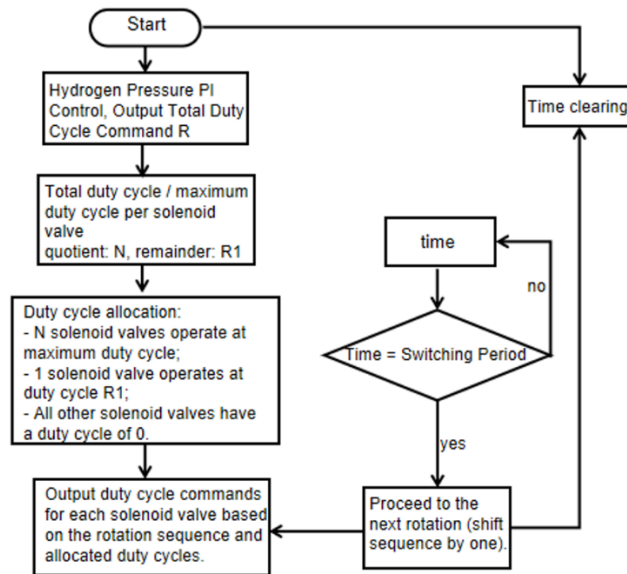


Figure 5. Control Flowchart.

The distribution method adopted in this paper, as shown in Figure 5, involves sequentially driving solenoid valves. After one valve completes its full duty cycle output, the next valve is activated. The full duty cycle duration for each valve can be adjusted based on control requirements and solenoid valve status. Based on the designed cycle duration, the duty cycles of each hydrogen injection valve rotate sequentially. The rotation order is shown in Table 2. This approach ensures control precision for low-flow requirements while reducing the overall switching frequency of solenoid valves. It also prevents uneven operational frequencies among valves, which could lead to premature failure of certain valves due to high-intensity operation. Consequently, this extends the system's service life and lowers maintenance costs.

**Table 2.**  
Cycling Example.

Cycle Duty Valve No.	Solenoid Valve 1	Solenoid Valve No. 2	Solenoid Valve No. 3	Solenoid Valve No. 4	Solenoid Valve No. 5	Solenoid Valve 6
First Cycle	A	B	C	D	E	F
Second Cycle	F	A	B	C	D	E
Third Cycle	E	F	A	B	C	D
Fourth Cycle	D	E	F	A	B	C
Fifth Cycle	C	D	E	F	A	B
Sixth Cycle	B	C	D	E	F	A
Seventh Cycle	A	B	C	D	E	F
...	Similarly, the duty cycle allocation for each cycle will rotate in the above sequence.					

In the rotation mode, the distribution effect of the PWM duty cycle (upper limit 86%) is shown in Figure 6.

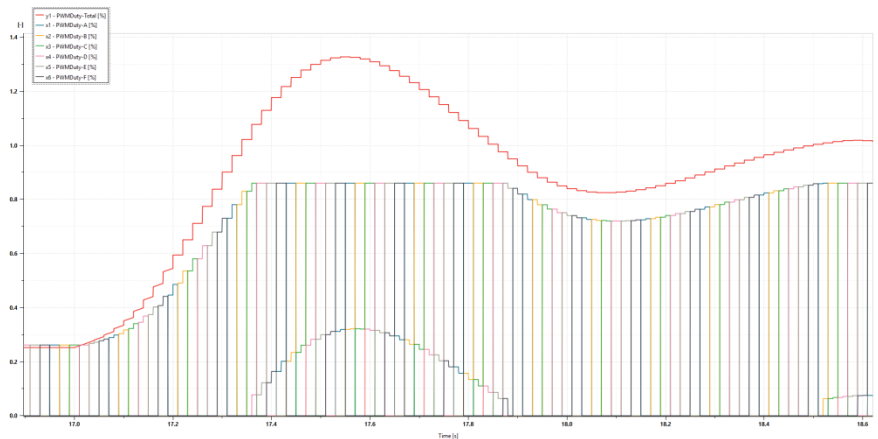


**Figure 6.**  
PWM Duty Cycle Cyclic Allocation Effect.

#### 4. Numerical Simulation

To validate the control performance of the above algorithm, a joint simulation model combining Simulink and AMESim was established. This leverages the strengths of each platform in control logic and physical modeling simulation, enhancing simulation effectiveness and efficiency. The Simulink model is shown in Figure 7, and the Amesim model is shown in Figure 8.

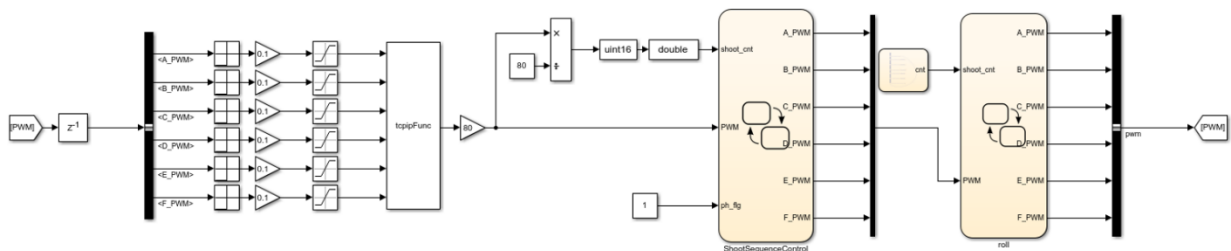


**Figure 7.**  
Simulink Model.

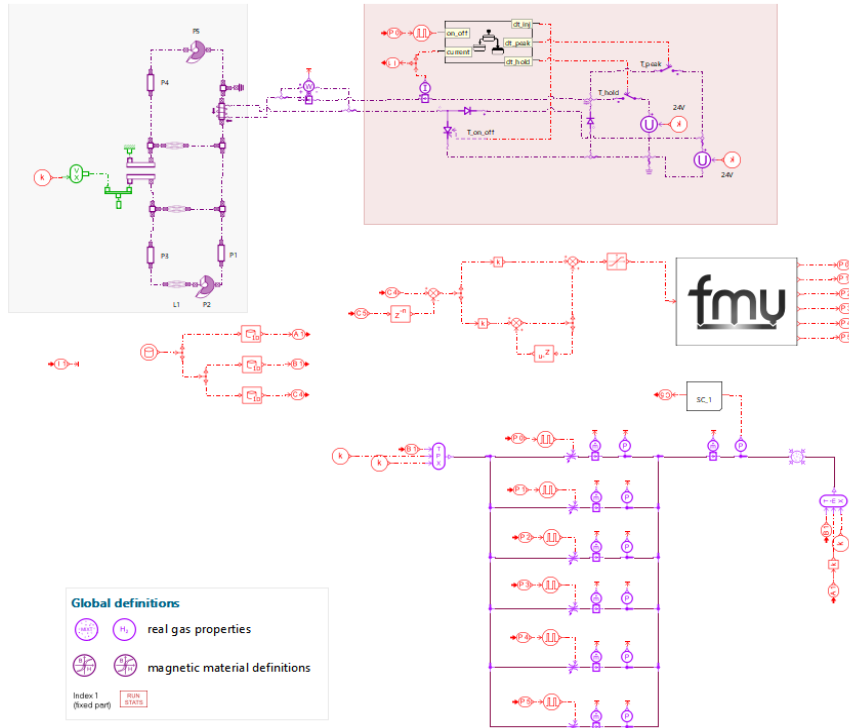


**Figure 8.**  
AMESim Model.

The Amesim module simulates the solenoid valves and hydrogen supply assembly, incorporating a PI module that outputs the total PWM duty cycle to Simulink. Simulink receives this overall duty cycle command, performs target duty cycle allocation and round-robin logic, then outputs target commands for the six solenoid valves to Amesim.

To investigate the impact of different power consumption and heat generation on solenoid valve lifespan under identical operating conditions when the model cannot run, a heat transfer model for the solenoid valve was established as shown in Figure 9.

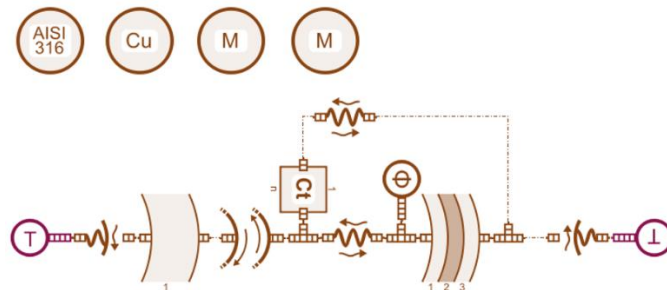


**Figure 9.**  
Solenoid Valve Heat Transfer Model.

#### 4.1. Hydrogen Pressure Control Comparison

The solenoid valve only drives the armature movement when the drive current exceeds the Peak current, meaning it operates only when the PWM command exceeds the Peak duty cycle. This characteristic causes fluctuations in hydrogen pressure and actual flow rate during low-flow demands if the duty cycle is distributed equally. Figure 10 compares the hydrogen pressure control effects of the distribution method described in this paper versus equal distribution.

The system requires 6 kW power, with a target hydrogen inlet pressure of 1.288 barA, a hydrogen flow rate of 0.09 g/s, and a target hydrogen inlet temperature of 333 K. In the figure, Pset represents the target hydrogen pressure, Pfb\_LD denotes the round-robin hydrogen pressure feedback, and Pfb\_JF indicates the equal-share hydrogen pressure feedback.

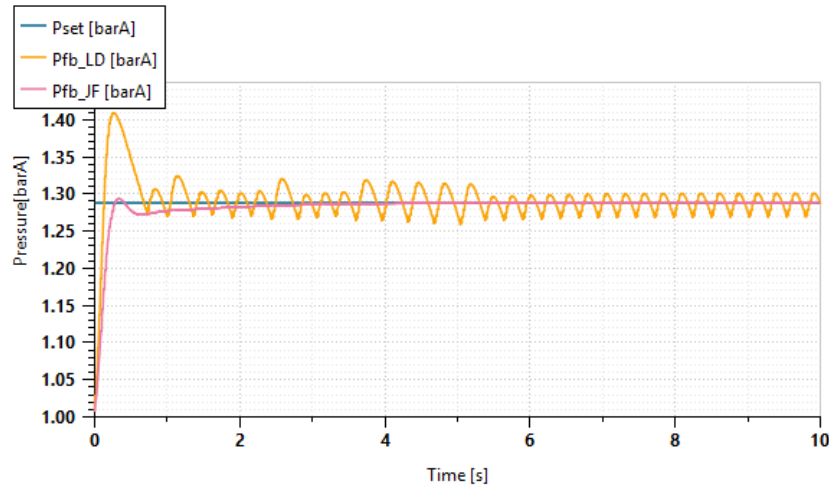


**Figure 10.**  
Comparative Diagram of Hydrogen Pressure Control Effectiveness.

#### 4.2. Cycling Performance

The solenoid valves used in this study have a design life of 600 million cycles. The fuel cell system design life is typically required to be 25,000 hours in the industry. The "Energy-saving and New Energy Vehicle Technology Roadmap 2.0" explicitly states that by 2035, the design life target for fuel cell engines used in buses and heavy-duty trucks should be  $\geq 25,000 - 30,000$  hours. Calculating based on 25,000 hours of engine operation and a solenoid valve PWM drive frequency of 50Hz, if the load is evenly distributed, each solenoid valve would require approximately 4.5 billion switching cycles. This far exceeds the design life of 600 million cycles, necessitating frequent solenoid valve replacements throughout the system's entire lifecycle.

To validate the algorithm presented herein, the fuel cell engine durability test method outlined in GB/Z 44116-2024—Fuel Cell Engine Durability Test Method was referenced. The standard specifies a single cycle duration of 1800 seconds. To enhance simulation efficiency, this study employs a 125kW system and reduces the runtime at each operating point to one-tenth of the standard duration. The simulation conditions are referenced in Figure 11.

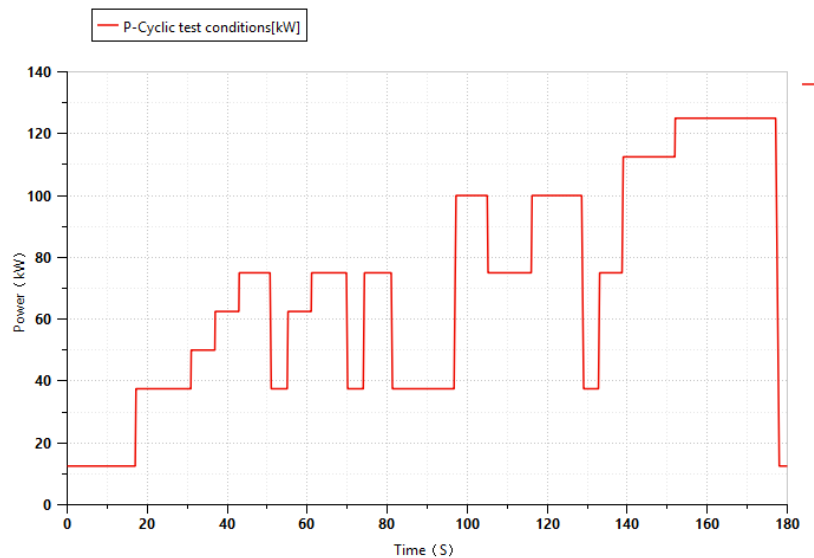


**Figure 11.**  
Simulation Conditions.

The co-simulation model was run under the above conditions. The switching counts for the equal-share, round-robin, and cyclic control methods over 180 seconds are shown in Figure 12. In equal-share mode, the six solenoid valves switched approximately 8,926 times. In the round-robin mode, the switching count for the first valve was similar to the equal-share mode but significantly higher than the cyclic mode. The switching counts for the second and third solenoids were also higher than in the cyclic mode. In the cyclic mode, all six valves had switching counts of approximately 3,730 cycles, substantially lower than in the equal-share mode.

Ignoring factors like temperature and humidity, and based on the solenoid valve's design life of 600 million cycles, converted to the system's full lifecycle (25,000 hours), the equal distribution mode requires replacing each of the 6 solenoid valves 6 times, totaling 36 replacements. In the rotating mode, more than 6 replacements are required, totaling 14 solenoid valves. In the cyclic mode, each of the 6 solenoid valves only needs to be replaced twice, totaling just 12 replacements. As

shown in Figure 13, Comparatively, the cyclic mode not only reduces the number of maintenance cycles but also decreases the quantity of solenoid valves requiring replacement.

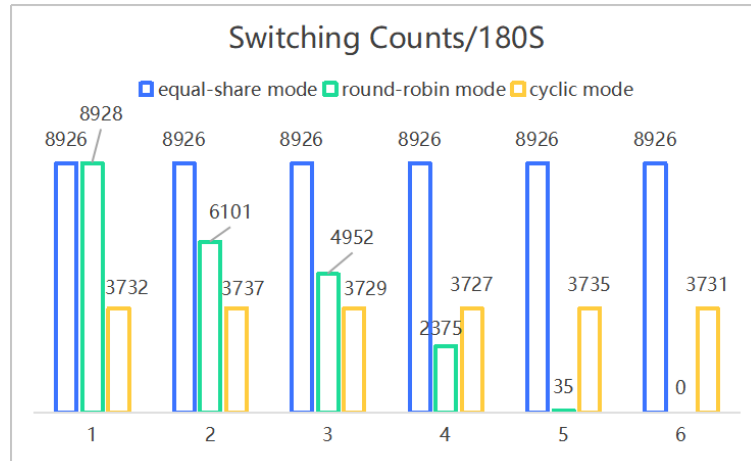


**Figure 12.** Comparison of Solenoid Valve Switching Frequency.

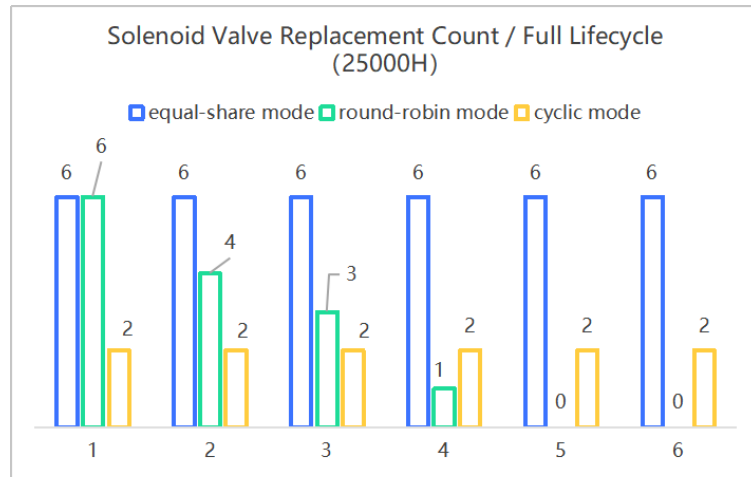


**Figure 13.** Comparison of Solenoid Valve Replacement Frequency.

Devices exposed to prolonged high-temperature and high-humidity environments accelerate aging and shorten their lifespan. The Parker model can be used for lifespan assessment. In the Parker model [11]:

$$AF = AF_H * AF_T = \left(\frac{H_A}{H_U}\right)^n * e^{\frac{E_a}{K_B} \left(\frac{1}{T_U} - \frac{1}{T_A}\right)} \quad (4)$$

Where:  $E_a$  - Activation energy (eV);  $K_B$  - Boltzmann constant ( $8.617385 \times 10^{-5}$  eV/K); T - Absolute temperature (K); H - Relative humidity (%RH); AF - Acceleration factor; Subscript A - Accelerated conditions; Subscript U - Operating conditions.

This paper disregards humidity effects. As shown in Equation (4), the greater the value of  $E_a$ , the more pronounced the temperature impact on lifespan. The primary failure modes for solenoid valves are electrical failure, mechanical failure, and seal failure. Empirical activation energies are typically 0.5–0.8 eV for electrical components, 1.0–2.5 eV for springs, and 0.7–1.0 eV for EPDM seals. To conservatively estimate temperature effects, this paper evaluates using an activation energy of 0.5 eV.

The temperature rise in solenoid valves primarily stems from coil power dissipation [5]:

$$q = \frac{Q}{V} = \frac{I^2 R}{V} \quad (5)$$

Where: q - heat per unit volume ( $J/m^3$ ); Q - joule heat (J); I - coil current (A); R - coil resistance ( $\Omega$ ); V - component volume ( $m^3$ ).

According to Fourier's law [12] the heat transfer rate between two media can be expressed as:

$$\dot{Q}_x = -kA \frac{\partial T}{\partial x} \quad (6)$$

$$\dot{Q}_y = -kA \frac{\partial T}{\partial y} \quad (7)$$

$$\dot{Q}_z = -kA \frac{\partial T}{\partial z} \quad (8)$$

Where:  $\dot{Q}_x, \dot{Q}_y, \dot{Q}_z$  —heat flux density in X,Y,Z directions (W);  $k$  —thermal conductivity (W/(m<sup>2</sup>·°C));  $A$ —cross-sectional area of component (m<sup>2</sup>); The negative sign indicates heat flow toward the direction of decreasing temperature.

The outer surface of the solenoid valve directly exposed to air constitutes the natural convection heat dissipation boundary. Thermal convection is described by Newton's cooling equation [12]:

$$Q = hA(T_s - T_a) \quad (9)$$

Where:  $Q$  - heat flux, W;  $A$  - component surface area (m<sup>2</sup>);  $h$  - convective heat transfer coefficient (W/(m<sup>2</sup>·°C));  $T_s$  - external surface temperature of the solenoid valve (°C);  $T_a$  - ambient temperature (°C).

Where:

$$h = \frac{k}{D} \left( 0.6 + \frac{0.387 R_a^{1/6}}{[1 + (0.559/P_r)^{9/16}]^{8/27}} \right)^2 \quad (10)$$

$$R_a = \frac{g B (\Delta T) D^3}{\eta \delta} g \quad (11)$$

In the equation:  $D$  - solenoid valve diameter (m);  $R_a$  - Rayleigh number;  $P_r$  - Prandtl number;  $g$  - gravitational constant (m<sup>2</sup>/s);  $B$  - thermal expansion coefficient (K<sup>-1</sup>);  $\eta$  - kinematic viscosity;  $\delta$  - thermal diffusion coefficient (m<sup>2</sup>/s).

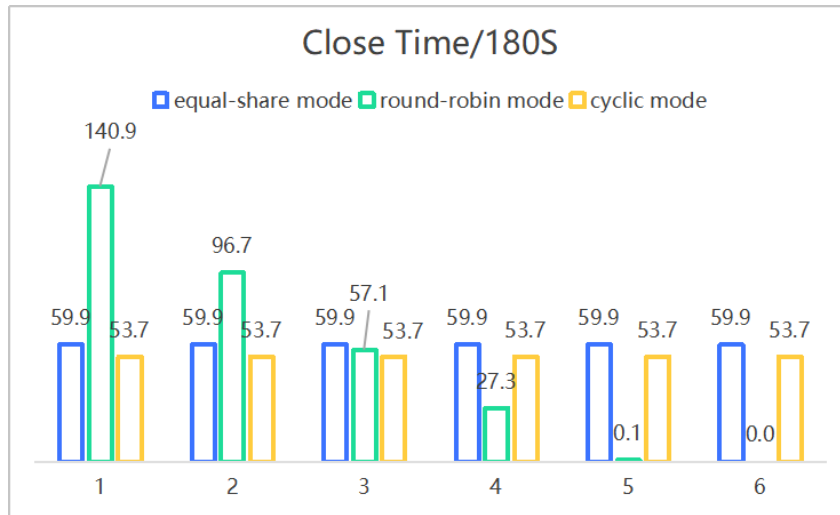


**Figure 14.** Comparison of Solenoid Valve Power Consumption.

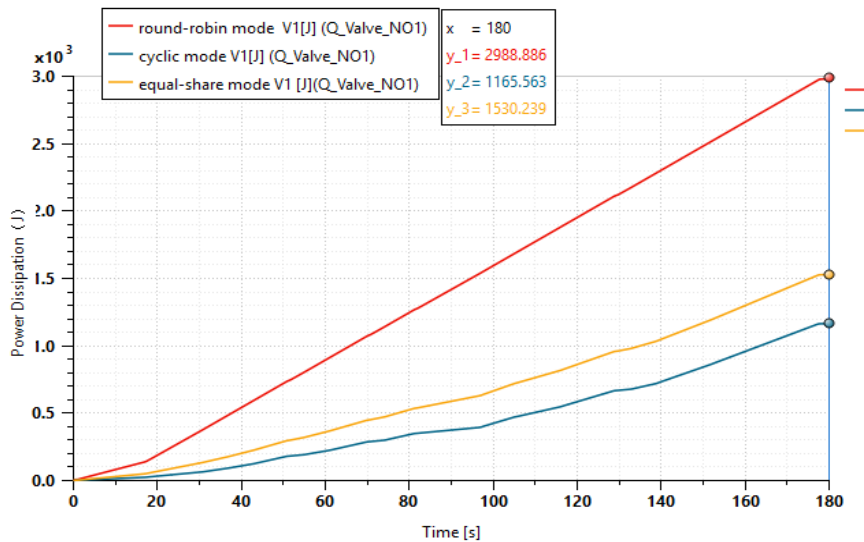


**Figure 15.** Comparison of Heat Generation in Three Modes.

Figure 14 compares the power consumption of the first solenoid valve under three operating modes. At the end of operating condition (180S) in Figure 11, the total heat generated was 1530 J in the equal-share mode, 2989 J in the rotating mode, and 1165 J in the cyclic mode, as shown in Figure 15. For simplified simulation, the heat generation power during the operating condition process is considered constant: 8.5 W in the equal-share mode, 16.6 W in the rotating mode, and 6.47 W in the cyclic mode. These values were then substituted into the model shown in Figure 9.

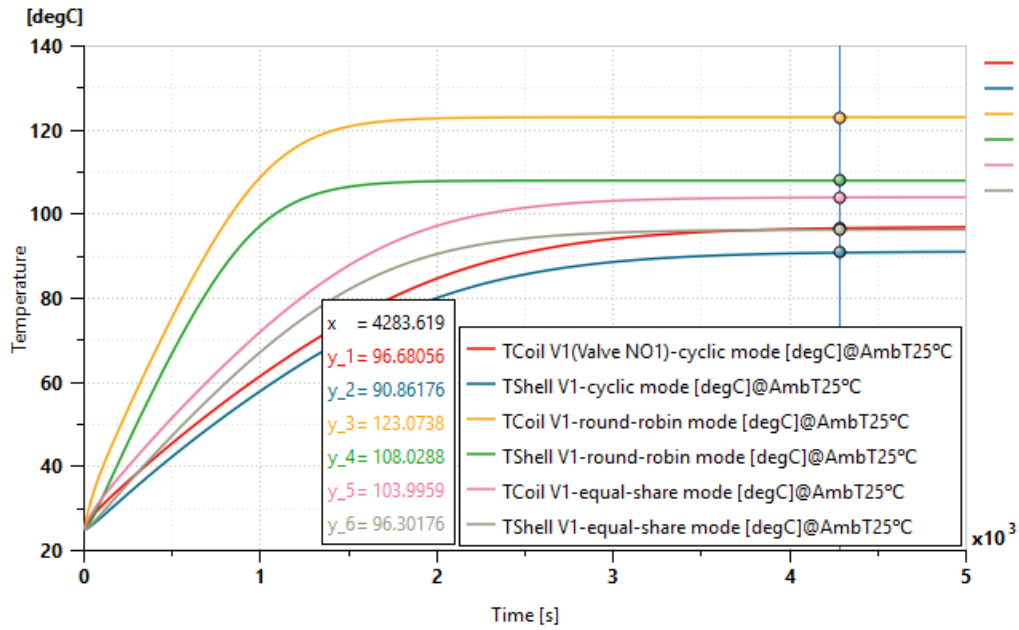


Figure 16. Comparison of Temperatures in Three Modes.

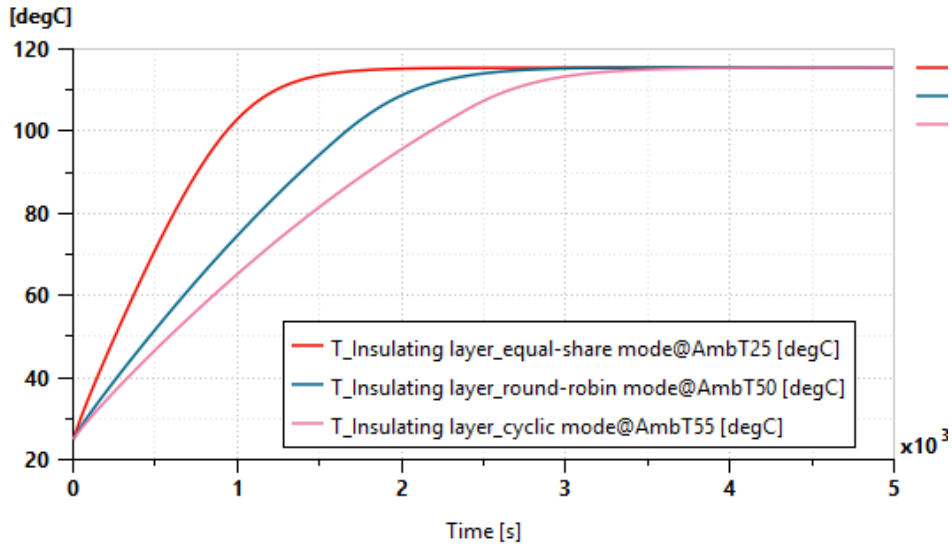


Figure 17. Schematic diagram of the operating conditions under three states.

As shown in Figure 16, after temperature stabilization, the coil and housing temperatures of the first solenoid valve in the rotating mode are significantly higher than those in the equal-sharing and cyclic modes, with the lowest temperature observed in the cyclic mode. As temperatures rise, the corresponding valve body lifespan decreases. As shown in Figure 17, Comparing insulation layer temperatures: operating in round-robin mode at 25°C ambient temperature, equal-share mode at 50°C ambient temperature, and cyclic mode at 55°C ambient temperature all result in a stable insulation layer temperature of 115°C. Thus, the insulation layer temperature of Solenoid Valve 1 operating in round-robin mode at 25°C ambient temperature is equivalent to that in cyclic mode at 55°C ambient temperature.

Referring to the Parker model in Formula 4, the acceleration factor at 55°C is 5.96 compared to 25°C. Thus, at 25°C ambient temperature, the insulation layer lifespan of Solenoid Valve 1 in cycling mode is reduced to 1/6th of that in cyclic mode. By extension, other solenoid valve components also experience accelerated aging due to higher temperatures in cycling and equal-share modes compared to cyclic mode. Consequently, under identical operating conditions, the overall lifespan of the solenoid valve is further reduced compared to cyclic mode.

### 5. Experimental Verification

To further verify the hydrogen pressure control effect of the polling mode and the service life performance of the hydrogen supply assembly under this mode, a test bench was designed and assembled to conduct the durability test of the hydrogen supply assembly. The schematic diagram of the test bench is shown in Figure 18, and the physical picture of the test bench is shown in Figure 19.

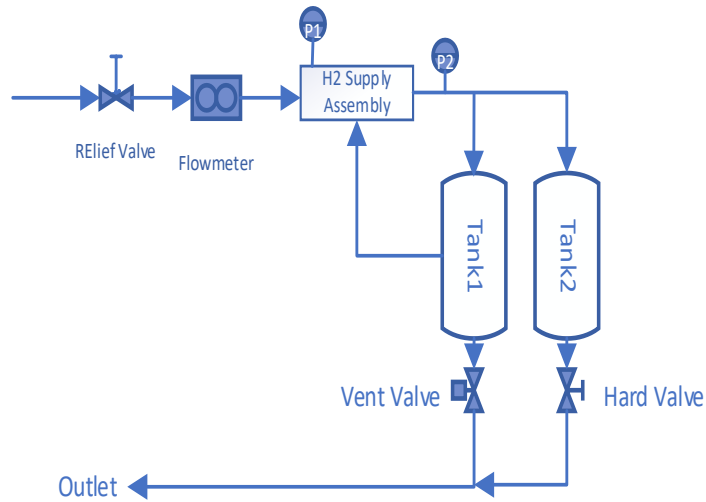


**Figure 18.**  
The schematic diagram of the test bench.

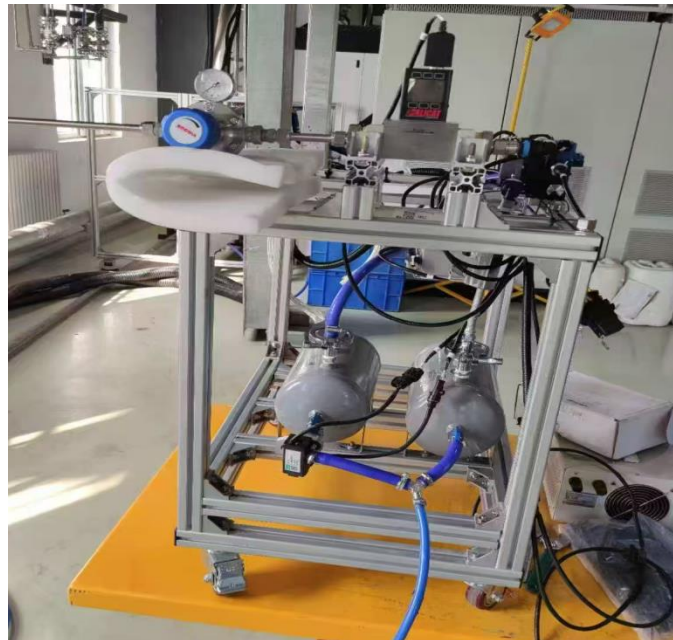


**Figure 19.**  
Test bench.

As shown in Figure 19, the test bench was built and the corresponding wiring harness was made. The front end was connected to the factory pipeline nitrogen with a pressure of 2.2 MpaA, and then the pressure was adjusted to the system inlet pressure of 1.5 MpaA (P1) through a Relief Valve. Tank 1 and Tank 2 were used to simulate the hydrogen cavity of the stack, and the Hard Valve was adjusted to simulate the stack consumption. The Vent Valve was used to simulate the water drainage action during the operation of the fuel system. A flow meter was connected in series at the front end of the hydrogen supply assembly to measure the actual gas flow rate, and the solenoid valve on the gas supply assembly was adjusted by the controller to make the output pressure P2 equal to the target stack inlet pressure under the working condition. The controller also performed data transmission with the upper computer to receive working condition instructions and record data through the upper computer.

To test the control effect under small flow rate, the controller was flashed with the equal distribution mode program, the target hydrogen inlet pressure of the stack was set to 1.29 barA, the Hard Valve was adjusted to make the gas flow rate 61 NLPM, and the response curve was recorded. Then, the polling mode program was flashed for comparison, as shown in Figure 20. The pressure fluctuation under the polling mode was significantly smaller than that under the equal distribution mode.

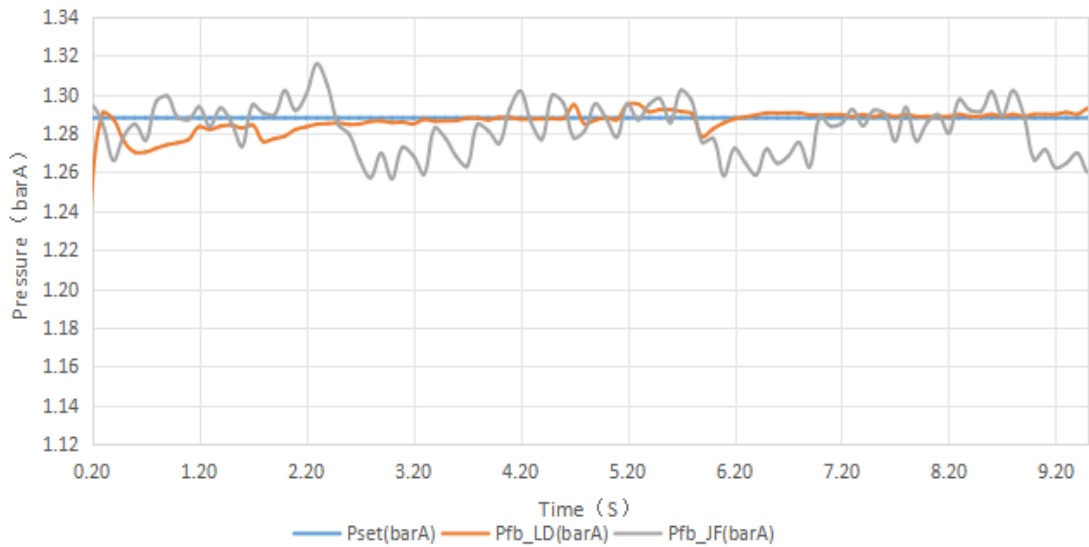


**Figure 20.**  
Comparison Diagram of Stack Inlet Pressure.

For the durability test, the Hard Valve was adjusted to a fixed angle, and the Vent Valve was kept normally closed. The operating conditions referred to *GB/Z 44116-2024—Test Method for Durability of Fuel Cell Engines*, which was converted into the hydrogen pressure requirements for each operating condition. The solenoid valve status was determined every 6 hours: each individual solenoid valve was given 0% and 100% opening degrees respectively, and it was measured whether the target stack inlet pressure P2 was normal. The experiment was terminated when two consecutive faults occurred in the two solenoid valves.

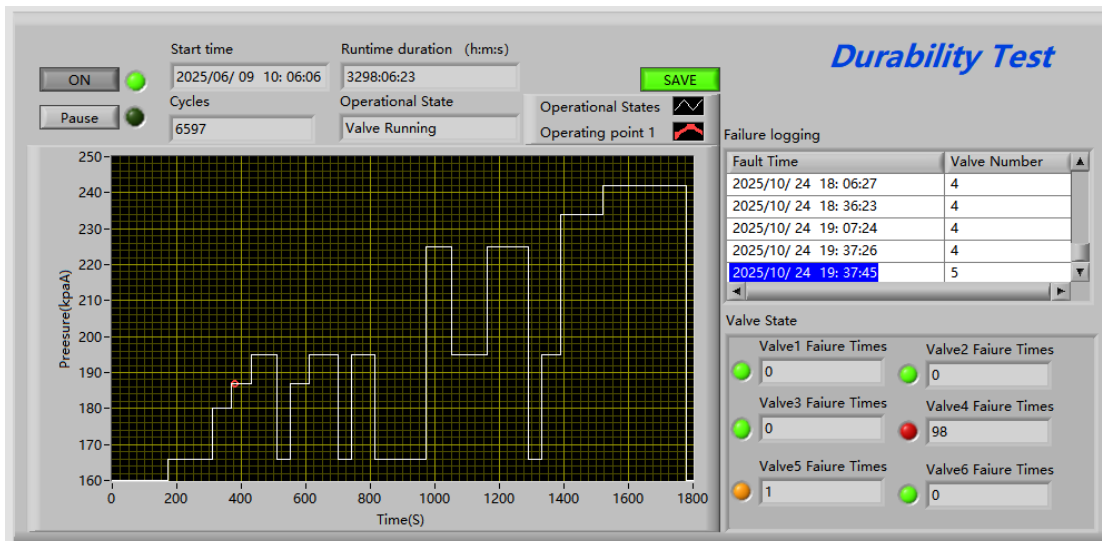


**Figure 21.**  
The upper computer monitoring interface.

Figure 21 shows the upper computer monitoring interface for the durability of the hydrogen supply assembly under the equal distribution mode. When running the 6597th operating condition cycle, Valve 4 had 16 faults and Valve 5 had 1 fault. The durability results of the equal distribution and polling modes are statistically summarized as follows. The Table 3 show that the polling mode can effectively increase the operating time of the hydrogen supply assembly and improve the reliability of the system.

**Table 3.**  
Comparison of durability results.

	Equal Distribution Mode	Polling Mode
Operating Time to First Fault (H)	3204	8472
Faulty Valve Number at First Fault	Valve 4	Valve 2
Total Operating Time at the End of Operation (H) (at least two valves detect faults two or more times)	3414	8748
Number of Faulty Valves	3	2

## 6. Conclusion

This paper focuses on the optimization of the service life of hydrogen injection solenoid valves and the precise control of hydrogen pressure. Through simulation analysis, experimental verification and theoretical calculation, the following core conclusions are drawn, clarifying the superiority and application value of the polling control strategy:

**Optimization of control effect:** Both the rotation mode and the polling mode can effectively solve the pressure fluctuation problem that occurs when the equal distribution mode is used for control under small flow demand.

**Improvement of valve service life:** Under reference operating conditions, when the hydrogen injection proportional valve assembly works in the traditional equal distribution mode, the number of on-off times of each solenoid valve is much greater than that of the polling mode designed in this paper, about 2.4 times; the rotation mode has the problem of uneven valve load distribution, where the front-end valves have too high usage frequency and temperature, accelerating aging. In contrast, the polling mode can achieve balanced load distribution among 6 valves, significantly reducing the on-off frequency, power consumption and operating temperature of a single valve. Combined with the evaluation of the Parker model, it can effectively extend the valve service life and reduce the number of valve replacements.

**Improvement of system reliability:** Durability test verification shows that the time to first failure (8472H) of the hydrogen supply assembly under the polling mode is much longer than that under the equal distribution mode (3204H), the total operating time at the end of operation (8748H) is more than 2.5 times that of the equal distribution mode (3414H), and the number of faulty valves is smaller, which greatly improves the reliability and durability of the hydrogen supply system and reduces the later maintenance cost.

Compared with the traditional equal distribution control mode, the hydrogen injection polling control scheme designed in this paper has significant advantages in hydrogen pressure control accuracy, valve service life optimization, system energy consumption control and other aspects. It can provide technical support for high-reliability fuel cell hydrogen supply systems and is suitable for scenarios such as commercial vehicles that have high requirements for fuel cell service life.

## References

- [1] International Energy Agency. Global Hydrogen Review, "Global hydrogen review," Retrieved: <https://www.iea.org/reports/global-hydrogen-review-2025>. 2025.
- [2] China Society of Automotive Engineers, *Technology roadmap for energy-saving and new energy vehicles 2.0*. Beijing: CSAE, 2021.
- [3] R. Guo, S. Li, and K. Tanaka, "A critical review on the solenoid valve reliability, performance and remaining useful life including its industrial applications," *Polymer Degradation and Stability*, vol. 208, p. 110245, 2023.
- [4] F. Liu and M. Zhou, "A model of sliding wear of ceramics," *Journal of Materials Engineering*, vol. 47, no. 4, pp. 112–120, 2019.
- [5] S. V. Angadi *et al.*, "Reliability and life study of hydraulic solenoid valve. Part 1: A multi-physics finite element model," *Engineering Failure Analysis*, vol. 16, no. 3, pp. 874-887, 2009, <https://doi.org/10.1016/j.engfailanal.2008.08.011>.
- [6] S. V. Angadi and R. L. Jackson, "A critical review on the solenoid valve reliability, performance and remaining useful life including its industrial applications," *Engineering Failure Analysis*, vol. 136, p. 106231, 2022, <https://doi.org/10.1016/j.engfailanal.2022.106231>.
- [7] H. Hou, G. Sun, B. Hao, J. Xia, B. Sun, and J. Wang, "Study on fatigue life evaluation method for control electromagnetic valve of locomotive braking system for rail transit," *Journal of Mechanical Engineering*, vol. 10, pp. 141–145, 2025.
- [8] J. Li, M. Xiao, and X. Tang, "Fault diagnosis of solenoid valves based on gradual failure of coils," *Journal of Engineering for Thermal Energy and Power*, vol. 33, no. 8, pp. 99-107, 2018.
- [9] G. Tao and Y. Ma, "Simulation calculation of fatigue life for high-speed response solenoid valve springs," *Hydraulics, Pneumatics & Seals*, vol. 6, pp. 11–12, 2003.
- [10] G. Mazaev, G. Crevecoeur, and S. Van Hoecke, "Bayesian convolutional neural networks for remaining useful life prognostics of solenoid valves with uncertainty estimations," *IEEE Transactions on Industrial Informatics*, vol. 17, no. 12, pp. 8418-8428, 2021, <https://doi.org/10.1109/TII.2021.3078193>.
- [11] Standardization Administration of the People's Republic of China, *GB/T 34986-2017: Methods for product accelerated testing*. Beijing, China: National Standard, 2017.
- [12] B. Li, Z. He, and X. Chen, *Design, simulation, and optimization with ANSYS workbench*. Beijing: Tsinghua University Press, 2011.